4776 *Organometallics* **1996,** *15,* 4776−4782

Structure of Lithium Bis(diphenylphosphino)amide: An X-ray, NMR, and Modeled Theoretical Study

Thomas Kremer,† Frank Hampel,† Falk A. Knoch,‡ Walter Bauer,†
Astrid Schmidt,‡ Peter Gabold,‡ Martin Schütz,‡ Jochen Ellermann,‡ and
Paul von Ragué Schleyer*,†

Institut für Organische Chemie, Universität Erlangen-Nürnberg, Henkestrasse 42, D-91054 Erlangen, Germany, and Institut für Anorganische Chemie, Universität Erlangen-Nürnberg, Egerlandstrasse 1, D-91058 Erlangen, Germany

Received June 10, 1996⊗

Monomeric lithium bis(diphenylphosphino)amide, $LiN(PPh_2)_2$ (**5**), solvated with tetrahydrofuran, **5**·3THF, was characterized by single-crystal X-ray analysis. The pentacoordinated lithium environment, a distorted trigonal bipyramid, includes two THF oxygens and the nitrogen of the bis(phosphino)amide in the equatorial positions; the third oxygen and a phosphorus are apical. ^{31}P and ^{6}Li NMR spectroscopy show that the monomeric structure of **5** in THF solution is similar to the X-ray structure of solid **5**·3THF. Dynamic ^{31}P NMR spectroscopy gave an 8.1 kcal/mol rotation barrier around the PN bonds. The ^{6}Li−CP/MAS spectrum of **5**·3THF has a single ^{6}Li line, whereas the ^{31}P CP/MAS spectrum reflects the chemical nonequivalence of the phosphorus sites observed by X-ray analysis. The appearance of two ^{31}P signals in the solid-state NMR spectrum at +25 °C suggests a minimum activation barrier of the P,P-exchange process of $\Delta G^{\ddagger} > 12.6$ kcal/mol in the solid state. *Ab initio* calculations on the simplified, unsolvated models, PH_2NH_2, $(PH_2)_2NH$, PH_2NH^-, $(PH_2)_2N^-$, PH_2NHLi, and $(PH_2)_2NLi$, show that the strong stabilization of the amino anions by the α-phosphino substituents is due to negative hyperconjugation and phosphorus polarization. The presence of the metal counteracts much of the α-substituent stabilizing effect in the free anions. The metal cations in lithiated model compounds show little tendency to bridge.

Introduction

Lithium organonitrogen compounds—particularly lithium amides (R_2NLi)—are widely used both in organic and in organometallic synthesis.[1−4] While X-ray structures and theoretical studies on "simple" lithium amides (i.e. those RR′NLi compounds where R and R′ contain no additional functionalities or heteroatoms) are now available,[4] studies on functionalized lithium amides like the phosphonium amides ($R_2PNR'Li$) considered in the present study are in general quite recent.[5]

A decade ago textbooks described the "P−N bond to be one of the most intriguing in chemistry and to elude a detailed satisfactory description."[6] Since the mean value of the PN bond length in unconstrained phosphinoamines (**1**) is 1.7 Å,[5b] resonance structures like **2b**, implying phosphorus d-orbital participation, were invoked to explain the short (ca. 1.6 Å) PN distances in anions **2**. In contrast, Trinquier's and Ashby's recent computational study on model phosphinoamide compounds (e.g. PH_2NH_2, PH_2NH^-) attributed such short PN bond distances mainly to hyperconjugation, *i.e.* some delocalization of the nitrogen N_p lone pair into the antisymmetrical combination of the empty PH_2 σ^* orbitals (as shown by **2c**).[5b]

(1) (2a) (2b)

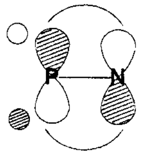

(2c)

The high polarizability of phosphorus provides additional stabilization, but the n(N) → d(P) interaction is not significant. The best depiction of a phosphinoamide anion is **2a**, with the negative charge mainly located on nitrogen.[5b]

In lithiated phosphinoamides the lone pair on phosphorus also can interact with the metal cation. Such interactions are apparent in the X-ray structure of dimeric lithium (phenylamino)diphenylphosphane, [Li-

---

† Institut für Organische Chemie.

‡ Institut für Anorganische Chemie.

⊗ Abstract published in *Advance ACS Abstracts,* September 1, 1996.

[1] (a) Wakefield, B. J. *Organolithium Methods*; Academic Press: London, 1988. (b) Lambert, C.; Schleyer, P. v. R. In *Methoden der organischen Chemie (Houben-Weyl)*; Georg Thieme Verlag: Stuttgart, Germany, 1993; Bd. E19d (Carbanionen), S1.

[2] (a) Brandsma, L.; Verkruijsse, H. *Preparative Polar Organometallic Chemistry 1*; Springer: Berlin, 1987. (b) Brandsma, L. *Preparative Polar Organometallic Chemistry 2*; Springer: Berlin, 1990.

[3] Fieser, M. *Reagents for Organic Synthesis*; Wiley-Interscience: New York, 1990; Vol. 15 and earlier volumes give specific uses of lithium amides arranged according to individual N−Li compounds.

[4] (a) Gregory, K.; Schleyer, P. v. R.; Snaith, R. *Adv. Inorg. Chem.* **1991**, *37*, 47. (b) Mulvey, R. E. *Chem. Soc. Rev.* **1991**, *20*, 167. (c) Sapse, A. M.; Schleyer, P. v. R. *Lithium Chemistry*; Wiley-Interscience: New York, 1995.

[5] (a) Ashby, M. T.; Li, Z. *Inorg. Chem.* **1992**, *31*, 1321. (b) Trinquier, G.; Ashby, M. T. *Inorg. Chem.* **1994**, *33*, 1306.

[6] Greenwood, N. N.; Earnshaw, A. *Chemistry of the Elements*; Pergamon Press: Oxford, U. K., 1984; p 619.

S0276-7333(96)00467-0 CCC: $12.00

$(PhNPPh_2)(OEt_2)]_2$ (shown schematically in **3**), where N, Li and P form distorted triangles.[5]

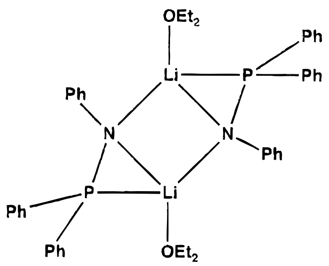

(3)

The charge localizing effects of lithium counterions and the structures and stabilities of α-heterosubstituted organolithium compounds have been studied computationally by Schleyer and co-workers.[7] While second-row heteroatoms (X = PH_2, SH, Cl) in $LiCH_2X$ show little tendency to interact with the lithium, α-NR_2-, OR-, and F-substituted organolithiums are strongly bridged. The latter compounds are 5−10 kcal/mol more stable than the free anions (based on $XCH_2^- + CH_3Li \rightarrow XCH_2Li + CH_3^-$). Hyperconjugative and polarization stabilization by second row substituents SiH_3, PH_2, SH, and Cl are strongly reduced in the corresponding organolithium compounds (compare eqs 1−4).

$$NH_2^- + PH_2NH_2 \longrightarrow NH_3 + PH_2NH^- \quad -27.3 \text{ kcal/mol} \qquad (1)$$

$$NH_2^- + PH_2NHPH_2 \longrightarrow NH_3 + PH_2NPH_2^- \quad -47.3 \text{ kcal/mol} \qquad (2)$$

$$LiNH_2 + PH_2NH_2 \longrightarrow NH_3 + PH_2NHLi \quad -11.3 \text{ kcal/mol} \qquad (3)$$

$$LiNH_2 + PH_2NHPH_2 \longrightarrow NH_3 + PH_2NLiPH_2 \quad -16.5 \text{ kcal/mol} \qquad (4)$$

As Li^+ gegenions tend to localize negative charge due to strong electrostatic interactions, significant energetic and structural effects on lithium phosphinoamides, relative to the free anions, are found.[7] For example, *ab initio* calculations (Becke3LYP/6-311++G(2d,2pd)//MP2-(full)/6-31++G** + ΔZPE(6-31+G*)) on the global minima for each species in eqs. 1−4 show that ion pairing destabilizes phospinoamines by large amounts, relative to the free phosphinoamine anions. The presence of Li^+ counterions competes with the stabilizing effect of the PH_2 group, due to electrostatic polarization of the nitrogen lone pairs.[7a]

NH_3 has a pyramidal ground state but a relatively low inversion barrier. The degree of pyramidalization at nitrogen, denoted as ΔΦ(N), is obtained by subtracting the sum of the three bond angles at N from 360°; ΔΦ(N) is 39.6° for NH_3, and the experimental barrier of inversion $\Delta E = 5.2$ kcal/mol.[8a] A single PH_2 on nitrogen reduces the pyramidalization and the inversion barrier: ΔΦ(N) is 13.9° for PH_2NH_2, and ΔE = 0.6 kcal/mol.[8b] As we will see in the theoretical part of this paper, with two PH_2 groups (*e.g.* $(PH_2)_2NH$ (**10**)) nitrogen is planar. In a fundamental *ab initio* study, Reed and Schleyer demonstrated that such nitrogen planarity is due to a combination of electronegativity (σ effects)[7c] and a strong n(N) → σ*(PH_2) interaction (anomeric effect or negative hyperconjugation).[8b]

Bis(phosphino)amines ($R'_2PNRPR'_2$) with essentially planar nitrogen environments might adopt three different conformations **4a** (C_s), **4b** (C_{2v}), and **4c** (C_{2v}). In each, the lone pairs on N and P are orthogonal. NMR, electron, and X-ray diffraction analyses, as well as molecular modeling, show that configuration **4c** is favored when R and R′ groups are relatively small (e.g., bis(diphenylphosphino)amine, R = H, R′ = Ph), but when the R and/or R′ substituents are large, **4a** is favored (e.g. R = iPr, R′ = Ph). Conformation **4b** has not been observed, evidently due to the repulsive interactions of the R′ groups.[9]

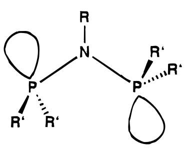

(4a)

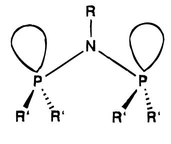

(4b)

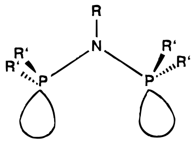

(4c)

Lithium bis(diphenylphosphino)amide, $LiN(PPh_2)_2$ (**5**),[10] an important precursor in phosphazane chemistry,[11] is known to be monomeric in THF solution.[10b] We describe the X-ray structure of **5**·3THF in the present paper. Solid-state CP/MAS NMR spectra of **5**·3THF and NMR studies of **5** in THF solution are compared, in order to establish the nature of the species in solution.

Ab initio calculations are now well accepted to study structures and mechanisms of polar organometallic compounds.[12,13] Since the X-ray structure of the neutral bis(diphenylphosphino)amine (**6**) is known,[14c] we performed high level *ab initio* calculations on simplified unsolvated models (PH_2NH_2, $(PH_2)_2NH$, PH_2NH^-, $(PH_2)_2N^-$, PH_2NHLi, $(PH_2)_2NLi$), to understand the

---

(7) (a) Schleyer, P. v. R.; Clark, T.; Kos, A. J.; Spitznagel, G. W.; Rohde, C.; Arad, D.; Houk, K. N.; Rondan, N. G. *J. Am. Chem. Soc.* **1984**, *106*, 6467. (b) Schleyer, P. v. R.; Jemmis, D. E.; Spitznagel, G. W. *J. Am. Chem. Soc.* **1985**, *107*, 6393. (c) Schleyer, P. v. R. *Pure Appl. Chem.* **1987**, *59*, 1647. (d) Schade, C.; Schleyer, P. v. R. *Adv. Organomet. Chem.* **1987**, *27*, 169. (e) El-Nahas, A.; Schleyer, P. v. R. *J. Comput. Chem.* **1994**, *15*, 596.

(8) (a) Allen, W. D.; East, L. G.; Csaszan, A. G. *Structures and Conformations of Non-Rigid Molecules*; Kluwer Academic Publishers: Amsterdam, 1993. (b) Reed, A.; Schleyer, P. v. R. *Inorg. Chem.* **1988**, *27*, 3969.

(9) Prout, T. R.; Imiolczyk, T. W.; Barthelemy, F.; Young, S. M.; Haltiwanger, R. C.; Normam, A. D. *Inorg. Chem.* **1994**, *33*, 1306 and references cited therein.

(10) (a) Schmidbaur, H.; Wagner, F. E.; Wohlleben-Hammer, A. *Chem. Ber.* **1979**, *112*, 496. (b) Ellermann, J.; Lietz, M. *Z. Naturforsch.* **1980**, *35b*, 64.

(11) (a) Witt, M.; Roesky, H. W. *Chem. Rev.* **1994**, *94*, 1163. (b) Ellermann, J.; Sutter, J.; Knoch, F. A.; Moll, M. *Angew. Chem., Int. Ed. Engl.* **1993**, *32*, 700. (c) Ellermann, J.; Sutter, J.; Schelle, C.; Knoch, F. A.; Moll, M. *Z. Anorg. Allg. Chem.* **1993**, *619*, 2006. (d) Ellermann, J.; Sutter, J.; Knoch, F. A.; Moll, M.; Bauer, W. *Z. Naturforsch.* **1994**, *49b*, 1763. (e) Ellermann, J.; Gabold, P.; Schelle, C.; Knoch, F. A.; Moll, M.; Bauer, W. *Z. Anorg. Allg. Chem.* **1995**, *621*, 1832.

(12) Hehre, W. J.; Radom, L.; Schleyer, P. v. R.; Pople, J. A. *Ab Initio Molecular Orbital Theory*; Wiley: New York, 1986.

(13) (a) Kaufmann, E.; Schleyer, P. v. R.; Houk, K. N.; Wu, Y.-D. *J. Am. Chem. Soc.* **1985**, *107*, 5560. (b) McKee, M. L. *J. Am. Chem. Soc.* **1987**, *109*, 559. (c) Kaufmann, E.; Schleyer, P. v. R.; Gronert, S.; Streitwieser, A.; Halpern, M. *J. Am. Chem. Soc.* **1987**, *109*, 2553. (d) Kaufmann, E.; Schleyer, P. v. R. *J. Comput. Chem.* **1989**, *4*, 437. (e) Li, Y.; Paddon-Row, M. N.; Houk, K. N. *J. Am. Chem. Soc.* **1988**, *110*, 3684. (f) Kaufmann, E.; Sieber, S.; Schleyer, P. v. R. *J. Am. Chem. Soc.* **1989**, *111*, 121. (g) Kaufmann, E.; Sieber, S.; Schleyer, P. v. R. *J. Am. Chem. Soc.* **1989**, *111*, 4005. (h) Leung-Toung, R.; Tidwell, T. T. *J. Am. Chem. Soc.* **1990**, *112*, 1042. (i) Li, Y.; Paddon-Row, M. N.; Houk, K. N. *J. Org. Chem.* **1990**, *55*, 481. (j) Hommes, N. J. R. v. E.; Bühl, M.; Schleyer, P. v. R.; Wu, Y.-D. *J. Organomet. Chem.* **1991**, *409*, 307. (k) Hommes, N. J. R. v. E.; Schleyer, P. v. R. *Angew. Chem., Int. Ed. Engl.* **1992**, *31*, 755. (l) Lambert, C.; Kaupp, M.; Schleyer, P. v. R. *Organometallics* **1993**, 12, 853. (m) Lambert, C.; Schleyer, P. v. R. *Angew. Chem., Int. Ed. Engl.* **1994**, *33*, 1129. (n) Kremer, T.; Harder, S.; Junge, M.; Schleyer, P. v. R. *Organometallics* **1996**, *15*, 585.

(14) (a) Ellermann, J.; Gruber, W. H. *Z. Naturforsch.* **1973**, *28b*, 310. (b) Nöth, H.; Meinel, L. *Z. Anorg. Allg. Chem.* **1967**, *349*, 225. (c) Nöth, H.; Fluck, E. *Z. Naturforsch.* **1984**, *39*, 744.

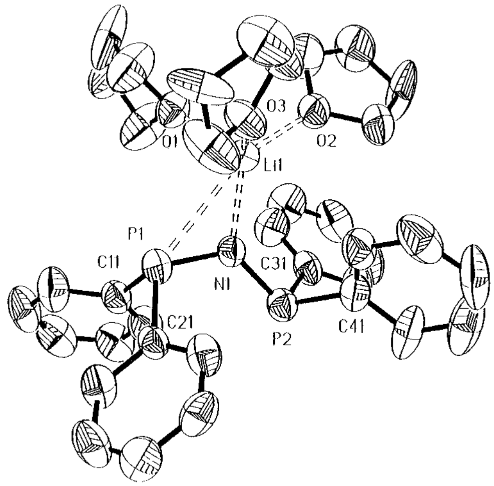

Figure 1. ORTEP plot of **5**·3THF. Thermal ellipsoids represent 50% probability, and hydrogen atoms have been omitted for clarity.

Table 1. Crystal Data and Structure Refinement for 5·3THF

empirical formula	$C_{36}H_{44}LiNO_3P_2$
fw	607.60
temp	200(2) K
wavelength	0.710 73 Å
cryst system	monoclinic
space group	$P2_1/n$
unit cell dimens	$a = 9.992(9)$ Å, $\alpha = 90°$; $b = 21.604(11)$ Å, $\beta = 103.27(8)°$; $c = 17.540(9)$ Å, $\gamma = 90°$
V	3685(4) Å^3
Z	4
D(calcd)	1.095 Mg/m^3
abs coeff	0.150 mm^{-1}
F(000)	1296
cryst size	0.50 × 0.40 × 0.40 mm
θ range for data collcn	2.23−25.26°
index ranges	$-11 \le h \le 11$, $-13 \le k \le 25$, $-21 \le l \le 21$
reflcns collcd	8909
indepdt reflcns	6634 ($R_{int} = 0.0977$)
refinement method	full-matrix least-squares on F^2
data/restraints/params	6634/2/428
goodness-of-fit on F^2	0.751
final R indices [$I > 2\sigma(I)$]	$R1 = 0.0733$, w$R2 = 0.1882$
R indices (all data)	$R1 = 0.2026$, w$R2 = 0.2413$
largest diff peak and hole	0.304 and −0.442 e Å^{-3}

Table 2. Selected Bond Lengths (Å) and Angles (deg) for 5·3THF

P(1)−N(1)	1.658(4)	P(1)−C(21)	1.853(5)
P(1)−C(11)	1.862(6)	P(1)−Li(1)	2.964(9)
N(1)−P(2)	1.686(4)	N(1)−Li(1)	2.030(1)
P(2)−C(41)	1.852(5)	P(2)−C(31)	1.866(5)
Li(1)−O(3)	1.969(9)	Li(1)−O(1)	1.995(9)
Li(1)−O(2)	2.010(10)		
N(1)−P(1)−C(21)	108.4(2)	N(1)−P(1)−C(11)	111.0(2)
C(21)−P(1)−C(11)	99.1(2)	N(1)−P(1)−Li(1)	41.0(2)
C(21)−P(1)−Li(1)	133.6(2)	C(11)−P(1)−Li(1)	122.4(2)
P(1)−N(1)−P(2)	124.7(3)	P(1)−N(1)−Li(1)	106.5(3)
P(2)−N(1)−Li(1)	128.7(4)	N(1)−P(2)−C(41)	104.0(2)
N(1)−P(2)−C(31)	102.1(2)	C(41)−P(2)−C(31)	97.9(2)
O(3)−Li(1)−O(1)	102.5(5)	O(3)−Li(1)−O(2)	101.5(4)
O(1)−Li(1)−O(2)	100.1(4)	O(3)−Li(1)−N(1)	113.1(5)
O(1)−Li(1)−N(1)	112.9(4)	O(2)−Li(1)−N(1)	124.0(5)
O(3)−Li(1)−P(1)	100.1(4)	O(1)−Li(1)−P(1)	88.5(3)
O(2)−Li(1)−P(1)	154.3(4)	N(1)−Li(1)−P(1)	32.4(2)

Table 3. Comparison of X-ray Geometries of 5·3THF and 6[a]

	5·3THF	**6**		**5**·3THF	**6**
PN	1.658(4) 1.686(4)	1.692(2)	CPC	99.1(2) 97.9(2)	not given
PC	1.835(5) 1.862(6) 1.866(5) 1.852(5)	1.827(4) 1.832(4)	CPN	111.0(2) 108.4(2) 102.1(2) 104.0(2)	104.0(1) 102.2(1)
NH		0.977(4)	LiNP	106.5(3) 128.7(4)	
NLi	2.030(10)		PNP	124.7(3)	118.9(2)
OLi	1.995(9) 1.969(9) 2.010(10)		PLi	2.964(9) 3.354	

[a] Reference 14c.

structural as well as energetic changes caused by the lithiation of phosphinoamines.

Results and Discussion

We synthesized **5** from bis(diphenylphosphino)amine, $HN(PPh_2)_2$ (**6**),[14] and n-BuLi[10a,b] in benzene; the white precipitate can be recrystallized from THF, to give colorless crystals of **5**·3THF.

X-ray Structure. As shown by the X-ray structure (Figure 1; see Tables 1 and 2 for details), **5**·3THF crystallizes as a monomer in the monoclinic space group $P2_1/n$.

The coordination sphere of lithium is a distorted trigonal bipyramid with N(1), O(1), and O(3) equatorial and P(1) and O(2) apical. The distances to the apical ligands are rather long. An additional THF molecule, incorporated in the crystal, has no contact to lithium. Indeed, isolated crystals tend to lose THF. Other monomeric solid-state structures of lithium amides are not common[4,15] and are limited to compounds with polydentate ligands or larger aromatic anions; dimerization or higher aggregation is prevented sterically. To the best of our knowledge, **5**·3THF is the first example of a distorted trigonal bipyramidal coordinated lithium amide monomer.

Since the X-ray structure of the neutral bis(diphenylphosphino)amine (**6**) is known,[14c] the structural changes due to metalation can be compared. Table 3 lists selected geometrical parameters of **5**·3THF and **6**. While **5**·3THF crystallizes in conformation **4a**, **6** adopts conformation **4c**. Upon metalation, the PN bonds are shortened whereas the PC bonds are elongated. Lithiation widens the PNP angle from 118.9 to 124.7°.

Structure in Solution. Figure 2 shows the ^{31}P NMR of **5** in THF-d_8 as a function of temperature. The single resonance at 30 °C ($\delta(^{31}\mathrm{P}) = 53.56$ ppm) is similar to that of other conformationally averaged, P symmetrical substituted bis(phosphino)amines.[9] Broadening of the ^{31}P signal is evident at −50 °C, and the coalescence temperature is reached at −80°; at −90 °C the signal splits into two equal area resonances, and at −100 °C the individual resonances of a "frozen" conformer are well resolved ($\delta(^{31}\mathrm{P}) = 53.17$ and 47.96 ppm). The ^{6}Li NMR shows only a single sharp resonance in the 30 to −111 °C temperature range, which indicates that only one species is present. We could not detect ^{31}P−^{6}Li or ^2J(PNP) coupling. ^2J(PNP) coupling constants depend markedly on the conformation of the PNP skeleton. Large positive ^2J(PNP) couplings are associated with the C_{2v} conformation of **4c**, whereas relative

---

(15) Olsher, U.; Izatt, R. M.; Bradshaw, J. S.; Dalley, N. K. *Chem. Rev.* **1991**, *91*, 137.

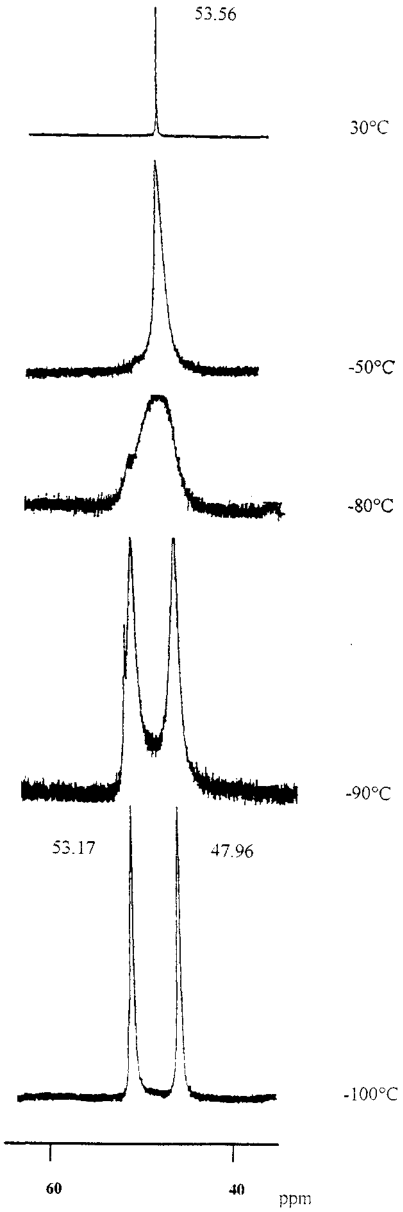

Figure 2. $^{31}P\{^1H\}$ NMR spectra of **5** in THF-d_8

small values are observed for C_s conformers of **4a**.[9] At −100 °C, the line widths of the ^{31}P signals preclude the detection of such small coupling constants.

The spectroscopic results and earlier colligative measurements[10b] suggest that **5** is monomeric in THF. The structure of **5** in THF solution should be similar to the X-ray structure of **5**·3THF. At −90 °C a dynamic process (*i.e.* rotation around PN bonds) is "frozen out". The activation barrier for this dynamic process is 8.1 kcal/mol at −80 °C (the coalescence temperature). For the dimeric lithium (phenylamino)diphenylphosphane, $[Li(PhNPPh_2)(OEt_2)]_2$ (**3**), the activation barrier for hindered rotation about P−N bond was found to be 7.5 kcal/mol by dynamic ^{31}P NMR spectroscopy.[5] The barriers of rotation around PN bonds in neutral bis(phosphino)amines with bulky N and P substituents are only slightly larger and range from 9.8 to 10.5 kcal/mol.[9] The smaller barrier in **5**·3THF is most probably due to the greater PNP angle compared to the neutral compounds which results in a greater distance between the substituents on the different phosphorus atoms.

Solid-State NMR. In agreement with the X-ray structure of **5**·3THF, the ^6Li CP/MAS spectrum of the crystals shows only a single peak at −1.53 ppm (Figure 3). The chemical shift is typical for lithium in such environments. A small impurity peak at 0.27 ppm in Figure 3 indicates traces of LiOH from hydrolysis. At the spinning speed employed (6.1 kHz) no rotational side bands are observed. Hence, both the chemical shift anisotropy and the quadrupole coupling constant, χ, of ^6Li must be well below this magnitude. This agrees with recent literature data for other lithium compounds.[16]

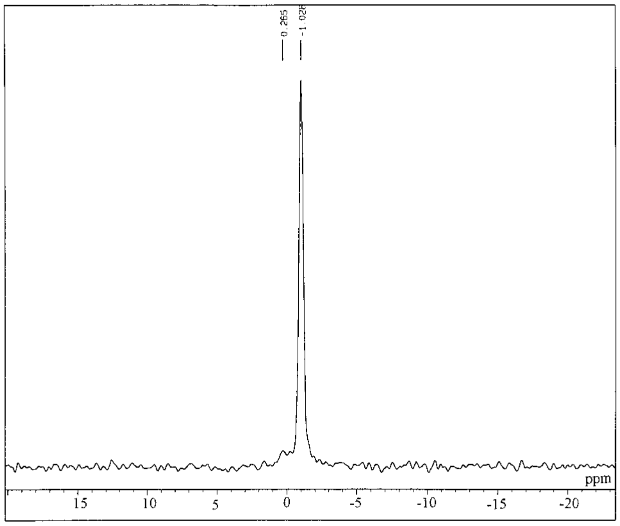

Figure 3. ^6Li CP/MAS spectrum of **5**·3THF (natural isotope abundance) at 11.7 T. The spinning speed is 6.1 kHz. For spectral parameters, see the Experimental Section.

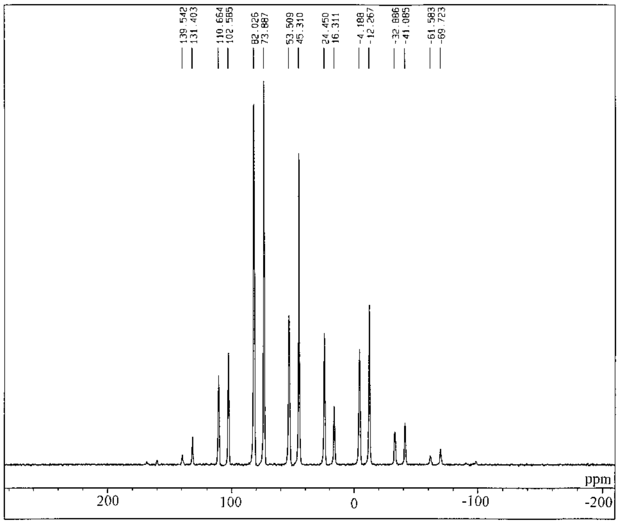

Figure 4. ^{31}P CP/MAS spectrum of **5**·3THF (natural isotope abundance) at 11.7 T. The spinning speed is 5.8 kHz. For spectral parameters, see the Experimental Section.

Quite interesting features are observed in the ^{31}P CP/MAS spectrum of **5**·3THF. Due to the inherently large chemical shift anisotropy of ^{31}P, the side bands in Figure 4 match the envelope of a powder pattern solid-state NMR spectrum. The different chemical environments of the two phosphorus sites in **5**·3THF result in two ^{31}P resonance lines at 53.51 and 45.31 ppm ($=\delta_{iso}$). These

---

[16] Espidel, I. E.; Harris, R. K.; Wade, K. *Magn. Reson. Chem.* **1994**, *31*, 166.

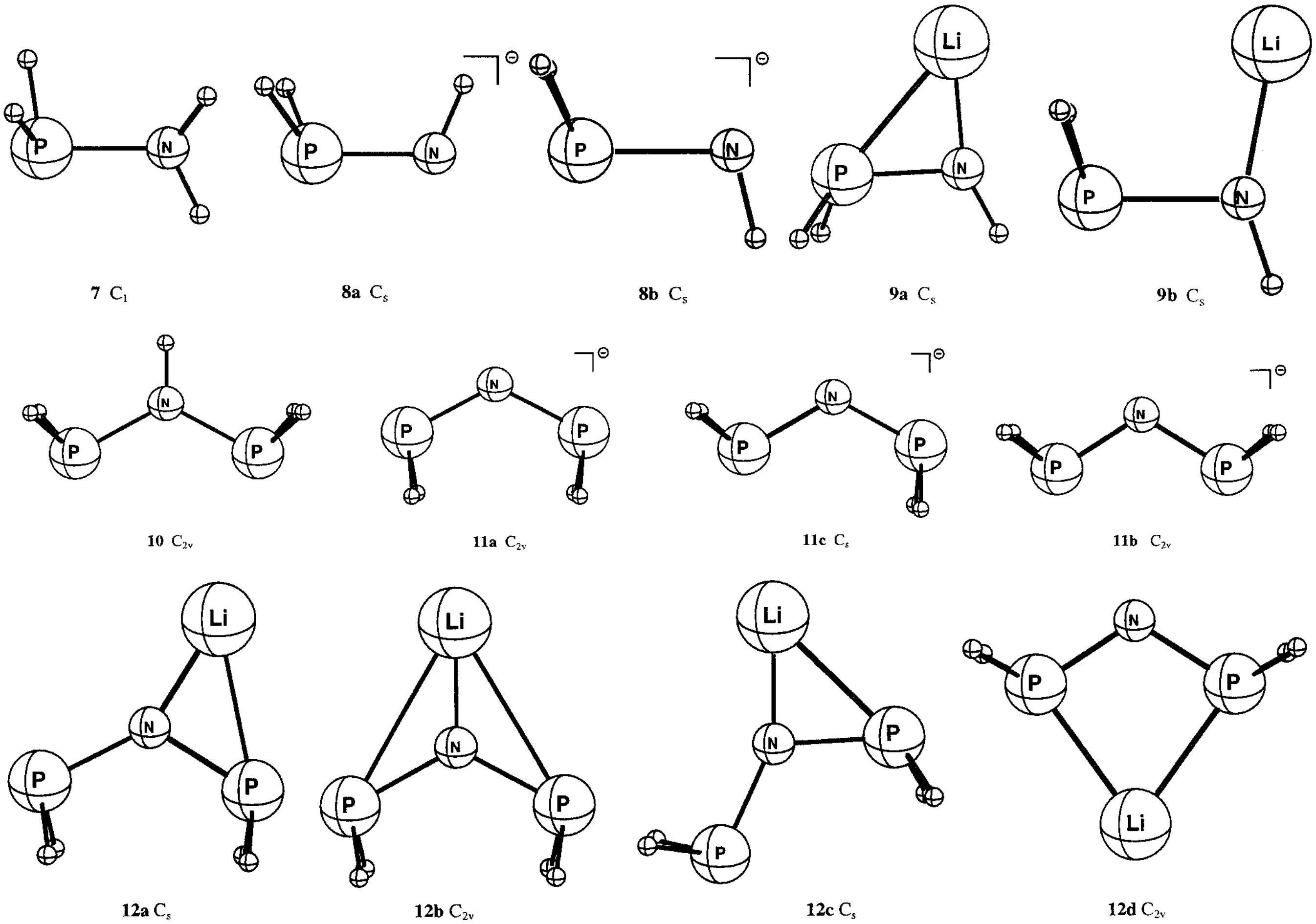
7 C_1 **8a** C_s **8b** C_s **9a** C_s **9b** C_s

10 C_{2v} **11a** C_{2v} **11c** C_s **11b** C_{2v}

12a C_s **12b** C_{2v} **12c** C_s **12d** C_{2v}

Figure 5. MP2-optimized molecules of the *ab initio* study.

shifts match those observed in solution at low temperatures (cf. Figure 2). As with the solution NMR, no $^{31}P,^{31}P$ coupling is observed (Figure 4). The appearance of two ^{31}P-signals in Figure 4 ($\Delta\nu = 1660$ Hz) indicates that the chemical exchange interconverting the two P atoms in **5**·3THF must be considerably slower in the crystal than in solution, where $\Delta G^{\ddagger}_{193} = 8.1$ kcal/mol. Since no coalescence of the two ^{31}P-signals occurs at room temperature, the activation barrier $\Delta G^{\ddagger}_{298}$ for the chemical exchange of the two ^{31}P-sites must well be above 12.6 kcal/mol in the solid state.

Computational Details. *Ab initio* calculations were performed using the Gaussian 92/DFT and Gaussian 94 program packages[17] on Convex C220, Cray YMP/832, and HP workstations. All geometries were optimized within the symmetries given both at RHF 6-31+G* and at MP2(full) 6-31++G** levels and characterized as minima or saddle points by calculation of vibrational frequencies at RHF/6-31+G*. Density functional theory[18] was employed to calculate the relative energies for the various isomers at Becke3LYP/6-311++G(2d,2pd) using the MP2-optimized geometries. Relative energies discussed below are at this level of theory and are corrected for differences in the RHF/6-31+G* zero point energies (scaled by 0.89).[12] Atomic charges and orbital interaction energies are obtained via the natural population analysis (NPA).[19]

Ab Initio Results. Figure 5 depicts the structures of the model phosphinoamines discussed in this study. Relative energies, charges, and selected geometrical parameters are given in Tables 4−6. Total and zero point vibrational energies are available as Supporting Information. Although our models (using H instead of C_6H_5 as substituents on P and ignoring solvation effects) are a rough simplification with respect to the molecules studied experimentally, they provide instructive information on the degree of lithium bridging, the preferred coordination site of the metal in ion-paired lithium phosphinoamines, and the geometric consequences of ion pairing.

---

(17) (a) Gaussian 92/DFT, Revision G.2. Frisch, M. J.; Trucks, G. W.; Schlegel, H. B.; Gill, P. M. W.; Johnson, B. G.; Wong, M. W.; Foresman, J. B.; Robb, M. A.; Head-Gordon, M.; Replogle, E. S.; Gomperts, R.; Andres, J. L.; Raghavachari, K.; Binkley, J. S.; Gonzalez, C.; Martin, R. L.; Fox, D. J.; Defrees, D. J.; Baker, J.; Stewart, J. J. P., and Pople, J. A. Gaussian, Inc., Pittsburgh, PA, 1993. (b) GAUSSIAN 94. Frisch, M. J.; Trucks, G. W.; Schlegel, H. B.; Gill, P. M. W.; Johnson, B. G.; Robb, M. A.; Cheeseman, J. R.; Keith, T.; Peterson, G. A.; Montgomery, J. A.; Raghavachari, K.; Al-Laham, M. A.; Zakrzewski, V. G.; Ortiz, J. V.; Foresman, J. B.; Cioslowski, J.; Stefanow, B. B.; Nanayakkara, A.; Challacombe, M.; Peng, C. Y.; Ayala, P. Y.; Chen, W.; Wong, M. W.; Andres, J. L.; Replogle, E. S.; Gomperts, R.; Martin, R. L.; Fox, D. J.; Binkley, J. S.; Defrees, D. J.; Baker, J.; Stewart, J. J. P.; Head-Gordon, M.; Gonzalez, C.; Pople, J. A. Gaussian, Inc., Pittsburgh, PA, 1995.

(18) (a) Ziegler, T. *Chem. Rev.* **1991**, *91*, 651. (b) Becke, A. D. *J. Chem. Phys.* **1993**, *98*, 1372, 5648. (c) Labanowski, J. W.; Andzelm, J. *Density Functional Methods in Chemistry*; Springer: New York, 1991. (d) Parr, R. G.; Yang, W. *Density Functional Theory of Atoms and Molecules*; Oxford University Press: New York, 1989. (e) Stephens, P. J.; Devlin, F. J.; Chabalowski, C. F.; Frisch, M. J. *J. Phys. Chem.* **1994**, *98*, 11623.

(19) (a) NBO analysis: Reed, A. E.; Curtiss, L. A.; Weinhold, F. *Chem. Rev.* **1988**, *88*, 899 and references cited therein. (b) NLMO bond orders: Reed, A. E.; Schleyer, P. v. R. *J. Am. Chem. Soc.* **1990**, *112*, 1434. (c) NPA charges: Reed, A. E.; Weinstock, R. B.; Weinhold, F. *J. Chem. Phys.* **1985**, *83*, 735.

Table 4. Relative Energies (kcal/mol)

	//RHF 6-31+G*	//MP2 (full) 6-31++G**	Becke3LYP 6-311++G (2D,2PD) //MP2 (full) 6-31++G**	Becke3LYP 6-311++G (2D,2PD) //MP2 (full) 6-31++G** + ΔZPE
8a (PH_2NH^-)	0.0	0.0	0.0	0.0
8b (PH_2NH^-)	1.1	0.4	0.8	0.9
9a (PH_2NHLi)	0.0	0.0	0.0	0.0
9b (PH_2NHLi)	3.1	5.3	4.1	3.8
11a ($(PH_2)_2N^-$)	0.0	0.0	0.0	0.0
11b ($(PH_2)_2N^-$)	4.7	5.1	4.5	4.7
11c ($(PH_2)_2N^-$)	3.1	3.9	3.0	2.7
12a ($(PH_2)_2NLi$)	0.0	0.0	0.0	0.0
12b ($(PH_2)_2NLi$)	0.2	1.9	1.2	1.0
12c ($(PH_2)_2NLi$)	2.6	2.4	1.8	1.7
12d ($(PH_2)_2NLi$)	19.0	18.3	12.3	12.9

Table 5. NPA Charges

	P	N	Li	H(P)	H(N)
7 (PH_2NH_2)	0.538	−1.144		−0.066	0.375
				−0.083	0.379
8a (PH_2NH^-)	0.469	−1.398		−0.185	0.298
8b (PH_2NH^-)	0.418	−1.396		−0.164	0.305
9a (PH_2NHLi)	0.413	−1.514	0.911	−0.009	0.361
9b (PH_2NHLi)	0.513	−1.571	0.944	−0.127	0.368
10 ($(PH_2)_2NH$)	0.575	−1.257		−0.070	0.387
11a ($(PH_2)_2N^-$)	0.506	−1.452		−0.140	
11b ($(PH_2)_2N^-$)	0.488	−1.457		−0.130	
11c ($(PH_2)_2N^-$)	0.486	−1.469		−0.122	
	0.518			−0.145	
12a ($(PH_2)_2NLi$)	0.441	−1.604	0.927	−0.067	
	0.550			−0.090	
12b ($(PH_2)_2NLi$)	0.509	−1.639	0.954	−0.083	
12c ($(PH_2)_2NLi$)	0.439	−1.600	0.922	−0.066	
	0.532			−0.081	
12d ($(PH_2)_2NLi$)	0.452	−1.378	0.725	−0.063	

PH_2NH_2 has been well studied; the C_1 structure **7** is the global minimum.[5b,8b] PH_2NH^- has two C_s minima **8a**,**b**. The PN bond is shorter in both the anions **8a**,**b** than in **7**, due to hyperconjugation.[5b] The cis form **8a** is only 0.9 kcal/mol more stable than **8b**. The energy difference is more pronounced in the lithiated isomers. The lithium-bridged cis form **9a,** which models the situation in the dimeric lithium (phenylamino)diphenylphosphane [Li(PhNPPh$_2$)(OEt$_2$)] (**3**),[5] is 3.8 kcal/mol more stable than **9b**. The nitrogen charges are larger than those in the free anions. This charge localizing effect of lithium is responsible for the PN bond lengthening relative to the free anion separations; nevertheless they are shorter than in **7**. The lone pair on phosphorus in η^2-bonded **9a** is oriented toward lithium; a short PLi distance of 2.395 Å results. In **9b** the Li−P (lone pair) interaction is absent, the PLi distance (2.642 Å) is longer and the LiNP angle is larger. The lack of coordination to Li in **9b** is partially compensated by polarization of the PH bonds (P + 0.513, H(P) −0.127 in **9b** vs P + 0.413, H(P) −0.009 in **9a**) and favorable four center ($H^-{-}P^+{-}N^-{-}Li^+$) charge alternation. The PN bond is polarized strongly in all free anions.

The neutral bis(phosphino)amine **10** has a single minimum with C_{2v} symmetry which resembles the C_2 X-ray structure of bis(diphenylphosphino)amine (**6**).[14c] As noted above, this conformation is favored by bis(phosphino)amines with small substituents. The corresponding anion has two C_{2v} minima, **11a**,**b**. The former is 4.7 kcal/mol more stable. As negative hyperconjugation (see structure **2c**) is more important in anti n(N)−σ(PH_2) conformations (in which σ* PH_2 is oriented toward the lone pair on nitrogen),[8b] the PH bonds in **11a** are 0.014 Å longer than in **11b**. The former adopts conformation **4b** with eclipsed substituents on P. With small substituents (e.g. H in our model compounds) steric effects are not important, but with large phenyl groups crowding destabilizes this conformation. Structure **11c** is not a minimum but might be favored with larger substituents on P for steric reasons. All the anions **11a**−**c** have shorter PN bond distances than the neutral bis(phosphino)amine **10**.

The η^2-bridged isomer **12a** is the global minimum for the lithiated bis(phosphino)amines. The η^1-bound **12b** is the transition structure for Li "flipping" from one P to the other. The small (1 kcal/mol) barrier indicates that the extra stabilization due to P−Li bridging is small. Indeed, the bridging P−Li distance of 2.964(9)

Table 6. Calculated Bond Length (Å) and Bond Angles (deg) at //MP2(full) 6-31++G**

	PN	PH	NH	NLi	PLi	HPH	HPN	HNP	LiNP	HNH	HNLi	PNP
7 (PH_2NH_2)	1.721	1.404	1.009			98.5	103.3	120.3		111.5		
		1.413	1.007				98.5	114.8				
8a (PH_2NH^-)	1.661	1.457	1.024			88.5	110.5	112.5				
8b (PH_2NH^-)	1.674	1.440	1.020			89.0	106.8	104.3				
9a (PH_2NHLi)	1.685	1.416	1.013	1.769	2.395	94.8	110.1	116.3	87.8		155.9	
9b (PH_2NHLi)	1.707	1.430	1.010	1.747	2.642	90.3	102.9	108.0	99.8		152.2	
10 ($(PH_2)_2NH$)	1.724	1.410	1.011			94.1	110.2	119.3				121.4
11a ($(PH_2)_2N^-$)	1.670	1.445				89.8	105.5					121.6
11b ($(PH_2)_2N^-$)	1.682	1.431				90.3	103.9					114.2
11c ($(PH_2)_2N^-$)	1.685	1.444				90.0	104.0					119.8
	1.667	1.430				90.6	108.1					
12a ($(PH_2)_2NLi$)	1.710	1.422		1.785	3.366	92.3	106.8		148.7			122.4
	1.694	1.416			2.437	94.9	101.7		88.9			
12b ($(PH_2)_2NLi$)	1.705	1.420		1.783	3.005	92.9	103.1		118.9			122.1
12c ($(PH_2)_2NLi$)	1.724	1.415		1.790	3.425	92.9	100.8		154.2			118.7
	1.692	1.414			2.402	95.1	108.8		87.2			
12d ($(PH_2)_2NLi$)	1.669	1.409		2.878	2.428	95.1	107.8		57.4			114.8

Å in the X-ray structure of **5**·3THF is rather long. Structure **12c** models the X-ray structure of **5**·3THF. As in the free anion **11c** (with H as substituent on P), conformation **12c** is a transition state rather than a minimum. The barrier to rotation of the PN bond of the uncomplexed phosphorus in **12c** is 1.7 kcal/mol. As in the free anions (**11**), crowding due to phenyl substituents on P is expected to favor **12c** over **12a**. The small preference for lithium bridging in the model systems suggests that the experimental barrier of 8.1 kcal/mol for PN bond rotation in solution is due to the steric demands of the phenyl substituents rather than the disruption of the P−Li interaction.

Both PN distances are equal in the neutral bis(diphenylphosphino)amine (**6**)[14c] (1.692(2) Å; see Table 3). In **5**·3THF the lithium-bridged PN bond (1.658(4) Å) is shortened by 0.034 Å relative to **6**, whereas the other PN bond distance is nearly unchanged (1.686(4) Å). In our model systems **10** and **12c**, the shortening (0.032 Å) due to the bridging lithiation is nearly the same (the other PN distance also is unchanged; see Tables 3 and 6).

Transition metal phosphazane complexes often exhibit structures in which the metal is complexed by both P lone pairs, as in **12d**.[11] Such coordination has not been observed experimentally with alkali metals. The Li and N charges in **12d** (where lithium has no contact to nitrogen) are strongly reduced with respect to **12a**. Although a minimum, the energy is 12.9 kcal/mol higher energy than **12a**; this mitigates against the observation of **12d**.

Summary

The solid-state structure of **5**·3THF appears to be retained in THF solution: **5**·3THF is monomeric with the lithium atom bent toward one phosphorus atom. Whereas the phenyl groups at this P atom are endo, the corresponding groups at the second P atom are exo. We suggest that rapid interconversions of the exo and endo phenyl groups, accompanied by simultaneous "switching" of lithium, with a barrier of 8.1 kcal/mol, occurs in THF solution. This process is slowed at −80 °C, and two ^{31}P NMR signals are observed. ^{31}P solid-state NMR indicates that both the activation barriers for P,N-bond rotation and for the lithium "switching" are much higher in the solid state than in solution: two ^{31}P CP/MAS signals are observed even at room temperature.

The tendency of lithium to bridge PN bonds in phosphinoamides is rather small energetically. The charge localizing effect of lithium, the polarizability of phosphorus, and negative hyperconjugation (*i.e.* lengthening of the PR bonds due to the delocalization of the nitrogen N_p lone pair into the antisymmetrical combination of the empty PR_2 σ^* orbitals) govern the structure of **5**·3THF and similar lithium phosphinoamides (*e.g.* **3**).

Experimental Section

All operations were performed in an atmosphere of purified argon using standard Schlenk and needle/septum techniques. Solvents were dried over Na/K alloy, and THF-d_8 was dried over Na/Pb alloy. A equimolar solution of *n*-Bu^{6}Li in hexane was added dropwise to a stirred solution of **6** in benzene at room temperature. A voluminous white precipitate formed, and stirring was continued for 1 h. The white precipitate was washed several times with cold benzene and used for the solution NMR studies.

The yellow solution obtained by dissolving the white precipitate in THF gave colorless needles of **5**·3THF, on standing overnight at −20 °C. These crystals were suitable for X-ray analysis and were used for the solid state NMR experiments.

Crystal data for **5**·3THF: $M_r = 607.60$; monoclinic; space group $P2_1/n$; $a = 9.992(9)$, $b = 21.604(11)$, $c = 17.540(9)$ Å; $\beta = 103.27(8)°$; $V = 3685(4)$ Å^3; $D_{calc} = 1.095$ Mg m^{-3}; $Z = 4$; $F(000) = 1296$; graphite-monochromated Mo Kα radiation ($\lambda = 0.710\,73$ Å); $T = 200(2)$ K. Data were collected with a Nicolet R3mV diffractometer on a crystal with the dimensions 0.5 × 0.4 × 0.4 mm using the ω scan method ($4.0° < 2\theta < 50.0°$). Of a total of 8909 collected reflections 6634 were unique and 2244 with $I > 2\sigma(I)$ observed. The structure was solved by direct methods using SHELXTL Plus 4.11. A total of 428 parameters were refined with all data by full-matrix least squares on F^2 using SHELXL93 (G. M. Sheldrick, Göttingen, Germany, 1993).[20] All non-hydrogen atoms were refined anisotropically; the hydrogen atoms were fixed in idealized positions using a riding model. The THF ligands and an additional free THF molecule exhibit disorder which could be dissolved using distance restraints. Final R values: $R1 = 0.0733$ ($I > 2\sigma(I)$) and $wR2 = 0.2413$ (all data) with $R1 = \Sigma|F_o - F_c|/\Sigma F_o$ and $wR2 = (\Sigma w(F_o^2 - F_c^2)^2/\Sigma w(F_o^2)^2)^{0.5}$; largest peak (0.304 e Å^{-3}) and hole (−0.442 e Å^{-3}). A summary of the crystal data is given in Table 1.

Further details of the crystal structure investigation are available on request from the Director of the Cambridge Crystallographic Data Centre, University Chemical Laboratory, Lensfield Road, GB-Cambridge CB2 1EW, U.K., by quoting the full journal citation.

Solution NMR spectra were recorded in THF-d_8 on a JEOL GX 400 spectrometer. Chemical shifts were referenced to TMS (indirectly via the solvent signal), external 85% H_3PO_4, and external 1 M LiBr/THF for ^{1}H, ^{31}P, and ^{6}Li, respectively. No corrections for bulk magnetic susceptibilities have been carried out.

Solid-state NMR spectra were recorded on a JEOL Alpha 500 spectrometer by using 6 mm rotors. Isolated crystals of **5**·3THF were employed; the crystals were carefully handled under reduced pressure in order to avoid loss of THF, powdered, and transferred to the rotor under argon. Representative spectral parameters are as follows.

Parameters for Figure 3 (^{6}Li CP/MAS spectrum): spectral width 20 kHz, 2048 sampling points, zero filled to 8k complex data points, 32 scans, recycle delay 20 s, acquisition time 0.1 s, 90° pulse for 5.8 μs, contact time 5 ms, spectrometer frequency 73.6 MHz, 1 Hz exponential line broadening, rotor speed 6.1 kHz; reference, LiOH·H_2O (0.00 ppm).

Parameters for Figure 4 (^{31}P CP/MAS spectrum): spectral width 100 kHz, 2048 sampling points, zero filled to 8k data points, 128 scans, recycle delay 7 s, acquisition time 0.02 s, 90° pulse for 7.0 μs, contact time 2 ms, spectrometer frequency 202.4 MHz, 10 Hz exponential line broadening, rotor speed 5.8 kHz; reference, $(NH_4)_2HPO_4$ (1.60 ppm).

Acknowledgment. This work was supported by the Deutsche Forschungsgemeinschaft, the Fonds der Chemischen Industrie, the Volkswagen Stiftung, and the Convex Computer Cooperation.

Supporting Information Available: Tables of atomic coordinates and *U* values, anisotropic thermal parameters, bond lengths and angles, and hydrogen atom parameters for **5**·3THF and total and zero point vibrational energies of the ab initio optimized molecules (7 pages). Ordering information is given on any current masthead page.

OM960467B

---

[20] Sheldrick, G. M. SHELXL-93, Göttingen, 1993.